On Mooney Viscosity and Mooney Stress Relaxation. I

L. C. E. STRUIK

DSM Research, P.O. Box 18, 6160 MD Geleen, The Netherlands

Received 9 September 1998; accepted 14 January 1999

ABSTRACT: Mooney relaxation is highly nonlinear, strongly differs from stress relaxation at small strains, and can be described by Wagner's nonlinear rheological model for polymer melts. In the practical evaluation, the Mooney Stress Relaxation slope is more accurate than quantities such as t_{80}. © 1999 John Wiley & Sons, Inc. J Appl Polym Sci 74: 1207–1219, 1999

Key words: Mooney viscosity; Mooney stress relaxation; elasticity; rubbers; rheology; linear viscoelastic theory; nonlinear Wagner constitutive model

INTRODUCTION

The Mooney Stress Relaxation test, described by Koopmann and Kramer[1] and normalized by ASTM,[2] is used more and more often to determine the elastic effects in the rheology of unvulcanized elastomers. The test is shown in Figure 1 and explained in the legend. Elastomers with high molecular weight, broad molecular weight distribution, and/or long-chain branching show much slower relaxation than good flowing elastomers of low molecular weight.

Attempts have been made (see, e.g., ref. 3) to describe Mooney Stress Relaxation by linear viscoelastic theory.[4] In view of the large strains (about 400), such attempts appear questionable and indeed, as shown in the next section, the theory is inadequate. The relaxation curve $M(t)$ strongly differs from the stress–relaxation modulus $G(t)$ at small strains. A more realistic theory, taking the nonlinear effects into account, is presented in the third section. It is based on Wagner's nonlinear model originally developed for polyethylene melts.[5–7] The third section describes the principles; a verification on the basis of experimental data is given in a Part II of this series.[8]

A practical point concerns the way in which the rough data of the Mooney Stress Relaxation test should be evaluated. Experiments reveal that the torque relaxation can be approximated by a power law:

$$M(t) = M_1 t^{-\alpha} \tag{1}$$

in which t is the time in seconds, M_1 is the torque at $t = 1$ s, and α is a constant exponent.

In the literature, a discussion arose as to which quantity should be used to characterize the relaxation. Some authors[9–11] prefer exponent α; others[12] propose the quantity t_{80}, as defined in Figure 1, and also, the surface area $A = \int M(t)\, dt$ below the relaxation curve $M(t)$ between the two fixed times t_1 and t_2 has been advocated.[2] Obviously, the three quantities are related one-to-one if eq. (1) were exact. However, eq. (1) is an approximation and the sensitivity to experimental errors may be different for the three quantities. A simple error analysis given in the fourth section reveals that, in general, slope a is the most accurate, whereas t_{80} is considerably less accurate.

INADEQUACY OF A LINEAR VISCOELASTIC DESCRIPTION OF MOONEY STRESS RELAXATION

The strain history shown in Figure 1 is a ramp between $t = -240$ s and $t = 0$:

Journal of Applied Polymer Science, Vol. 74, 1207–1219 (1999)
 CCC 0021-8995/99/051207-13

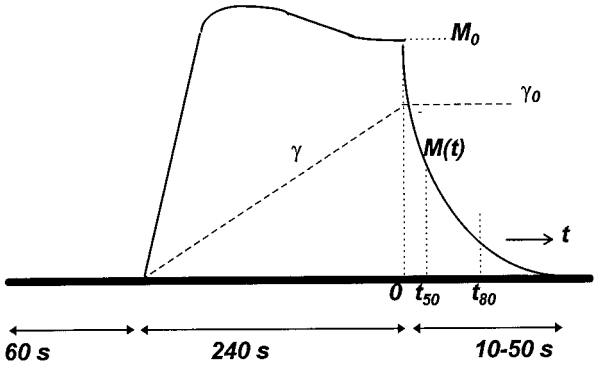

Figure 1 Outline of the Mooney Stress Relaxation test; for experimental details, including geometrical ones, see ref. 2; γ (dashed lines) denotes the prescribed shear strain, M (full curve), the measured torque. First, the sample is equilibrated for 60 s to the required temperature, without application of shear. Next, the sample is sheared at a constant rate for 4 min to a strain of about 400. Next, the shear strain is kept constant (γ_0) and the relaxation of $M(t)$ measured as a function of time t. Time t is taken zero at the moment of rotor stop (cessation of shearing). Usually the measuring period is only a few seconds to tens of seconds (i.e., much shorter than the original shearing time of 240 s). Thus, the times in the figure are not to scale; see arrows below the figure. The torque at the moment of rotor stop is denoted by M_0. Times t_{50} and t_{80} refer to the moments at which M had decreased to 50 and 20% of M_0, respectively. In the Mooney instrument, the shear strain is not constant but increasing from zero at the rotation axis to a maximum at the outside of the sample.[2] For simplicity, the present treatment is formulated for homogeneous shearing; corrections for the inhomogeneities can easily be made.[8]

$$\gamma = [t + t_1]q; \quad -t_1 < t < 0 \tag{2}$$

in which q is the strain rate and $t_1 = 240$ s is the straining period. Substitution into Boltzmann's superposition (linearity) integral immediately yields

$$M(t) = cq \int_0^{t_1} G(t + \tau)\, d\tau \tag{3}$$

where q is the strain rate (for $-t_1 < t < 0$), c is the geometrical factor determined by the instrument, $t_1 = 240$ s is the strain time, t is the time after cessation of shearing, and τ is the integration variable in time scale.

In the practical Mooney Stress Relaxation test, time t is always short compared to t_1 (e.g., with $t_1 = 240$ s and $t < 10$ s, we have $t/t_1 < 1/24 = 0.042$). According to eq. (3), $M(t)/[cqt_1]$ is the average value of all $G(t + \tau)$ values with τ between 0 and t_1. Since $t \ll t_1$, most of the $t + \tau$ values are much larger than t. For such $t + \tau$ values, $G(t + \tau)$ hardly depends on t because G generally varies slowly with the argument $t + \tau$, whereas $\tau \gg t$. (Note that $d \ln G(t + \tau)/d \ln t = -nt/(t + \tau)$, where n is the double-logarithmic slope of G for $t + \tau$.) Thus, the rapid relaxation of $M(t)$, shown in Figure 1, is impossible; the torque built up over 240 s cannot relax within 10 s. As an example, consider the case that $G(t)$ can be approximated by a power law:

$$G(t) = G_1 t^{-n} \tag{4}$$

At the temperatures where Mooney Stress Relaxation tests are done, exponent n of commercial elastomers ranges between 0.3 and 0.7.[8] Substitution of eq. (4) into (3) yields

$$M(t) = M_0[(1 + \zeta)^{1-n} - \zeta^{1-n}];$$

$$\zeta = t/t_1;$$

$$M_0 = cqG_1 t_1^{1-n}/(1 - n) \tag{5}$$

in which M_0 is the torque at $\zeta = 0$. Plots of $M(t)/M_0$ for various values of n are shown in Figure 2. For practical t/t_1 values (<0.05; see before), the relaxation is quite slow. The rapid relaxation found in actual Mooney tests is not reproduced, implying that the linear theory is inadequate.

In view of these results, Venneman's[3] theory, that links Mooney Stress Relaxation to the small-strain mechanical loss factor tan δ, must be considered inadequate. Indeed, tan δ generally correlates with the double-logarithmic slope of small-strain stress relaxation modulus $G(t)$ or dynamic modulus $G'(\omega)$[4]:

$$\tan \delta \approx -\tfrac{1}{2}\, \pi\, d \log G/d \log t$$

$$\approx \tfrac{1}{2}\, \pi\, d \log G'/d \log \omega \tag{6}$$

where $\log x$ is the 10-logarithm and $\ln x$ is the natural logarithm of x. However, these small-strain slopes are not simply related to the slope of

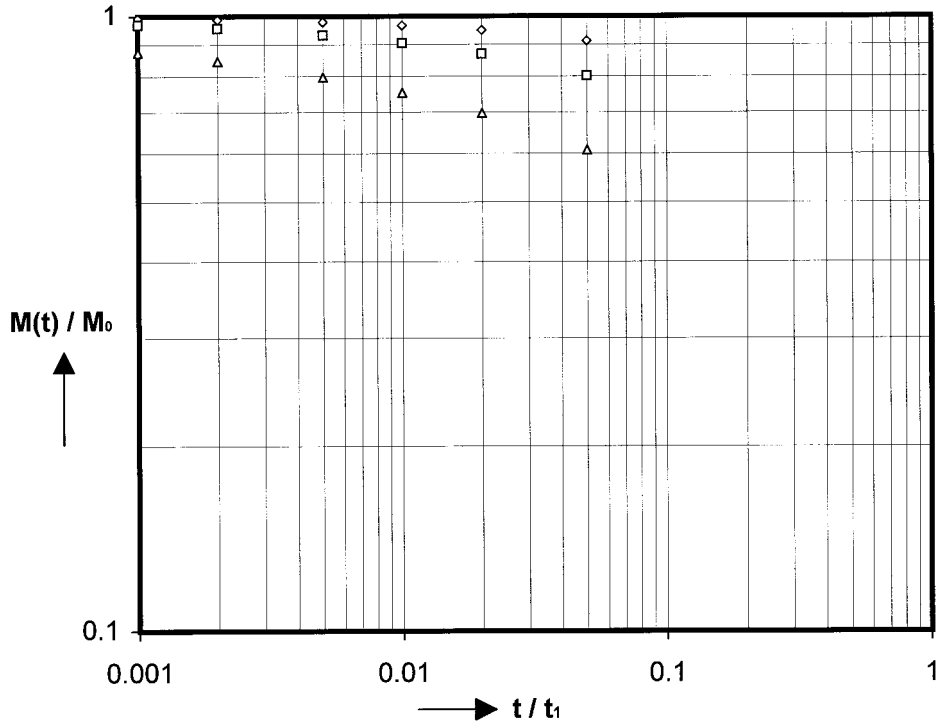

Figure 2 Mooney Stress Relaxation, $M(t)/M_0$, as calculated for a linear viscoelastic material with a stress–relaxation modulus according to eq. (4). Relevant n values for practical elastomers range between 0.3 and 0.7; symbols refer to $n = 0.3$ (◇), 0.5 (□), and 0.7 (△). In practical tests, time t remains short compared to straining time t_1 (e.g., $\zeta = t/t_1 < 0.05$). The figure shows only limited relaxation, certainly not the rapid relaxation down to about zero as shown by actual Mooney tests (c.f., Fig. 1). This demonstrates the inadequacy of the linear theory.

the (large-strain) Mooney Stress Relaxation (next section).

NONLINEAR THEORY OF MOONEY STRESS RELAXATION; APPLICATION OF WAGNER'S MODEL

The Wagner model[5–7] is an empirical generalization of Boltzmann's superposition principle. This description, although fully nonlinear viscoelastic, is limited to materials that do not fail during the Mooney test. For prescribed straining, starting at time $= -\infty$, the superposition principle says

$$\sigma(t) = \int_{-\infty}^{t} G(t-\xi)\dot{\gamma}(\xi)\, d\xi = \int_{-\infty}^{t} G(t-\xi)\{d[\gamma(\xi)-\gamma(t)]/\, d\xi\}\, d\xi = \int_{-\infty}^{t} \dot{G}(t-\xi)[\gamma(\xi)-\gamma(t)]\, d\xi \qquad (7)$$

in which γ is the shear strain, σ is used as a general symbol for stresses, including, in this case, shear stress, ξ is an integration variable on time t scale, and a dot denotes differentiation with respect to the argument, although it is assumed that $G_\infty = G\ (t = \infty) = 0$ (fluid).

Based on Lodge's temporary network theory for elastic fluids,[7] Wagner assumes that the nonlinearity can be described by a damping function h_s (index s stands for shear) that depends on the absolute value of $\gamma(\xi) - \gamma(t)$. Equation (7) is then replaced by:

$$\sigma(t) = \int_{-\infty}^{t} \dot{G}(t-\xi) \times h_s(|\gamma(\xi)-\gamma(t)|)[\gamma(\xi)-\gamma(t)]\, d\xi \qquad (8)$$

where $|x|$ denotes the absolute value of x.

By partial integration and with $G_\infty = 0$, eq. (8) changes into the alternative form of

$$\sigma(t) = -\int_{-\infty}^{t} h_s(|\gamma(\xi) - \gamma(t)|) \times [\gamma(\xi) - \gamma(t)]\, dG(t - \xi)$$

$$= \int_{-\infty}^{t} G(t - \xi)[d\{h_s(|\gamma(\xi) - \gamma(t)|) \times [\gamma(\xi) - \gamma(t)]\}/\, d\xi]\, d\xi \quad (9)$$

We now consider some special cases.

Step–Strain Stress Relaxation; Determination of the Damping Function[5–7]

We have $\gamma(t) = 0$ for $t < 0$ and $\gamma(t) = \gamma_0$ for $t \geq 0$ and apply eq. (8). Part of the integral for $\xi > 0$ disappears because $\gamma(t)$ then equals $\gamma(\xi) = \gamma_0$. For $\xi < 0$ and $t \geq 0$, we have $\gamma(\xi) - \gamma(t) = -\gamma_0$ [i.e., $\gamma(\xi) - \gamma(t)$ and $h_s(|\gamma(\xi) - \gamma(t)|)$ are constant and can be put outside the integral]. With $G_\infty = 0$, we get

$$\sigma(t) = -\gamma_0 h_s(\gamma_0) \int_{-\infty}^{0} \dot{G}(t - \xi)\, d\xi = \gamma_0\, h_s(\gamma_0) G(t) \quad (10)$$

Consequently, the apparent nonlinear stress–relaxation modulus $G_a(t) = \sigma(t)/\gamma_0$ equals the small-strain modulus, $G(t)$, multiplied by the damping function $h_s(\gamma_0)$. Since strain, γ_0, is constant, h_s is also constant and the same applies to ratio $G_a(t)/G(t)$:

$$G_a(t)/G(t) = h_s(\gamma_0) \quad (11)$$

Thus, we can find the damping function by measuring $G_a(t)$ at various values of γ_0. Experiments on polyethylene (PE)[7] reveal that h_s decreases exponentially with γ_0; the simplest description reads

$$h_s(\gamma_0) = \exp(-\mu\gamma_0) \quad (12)$$

with a coefficient μ of 0.1–0.2 for PE. A refined description uses two or more exponentials[5–8]; in the sequel we confine ourselves to eq. (12).

Mooney and Mooney Stress Relaxation Test

We now have (see Fig. 1)

$$\gamma(t) = 0 \quad \text{for } t < -t_1 \quad (13)$$

$$\gamma(t) = q(t + t_1) \quad \text{for } -t_1 < t \leq 0 \quad (14)$$

$$\gamma(t) = \gamma_0 \quad \text{for } t \geq 0;\ \gamma_0 = qt_1 \quad (15)$$

Mooney Test; Shearing Period; $-t_1 < t < 0$

For the period of shearing, eqs. (13)–(15) yield

$$\gamma(\xi) - \gamma(t) = \begin{cases} -q(t + t_1); & \xi < -t_1; \quad -t_1 < t < 0 \quad (16) \\ -q(t - \xi); & -t_1 < \xi < t; \quad -t_1 < t < 0 \quad (17) \end{cases}$$

We now apply eq. (9). For $\xi < -t_1$, $\gamma(\xi) - \gamma(t)$ and $h_s(|\gamma(\xi) - \gamma(t)|)$ do not depend on ξ and the integrant vanishes. Consequently,

$$\sigma(t') = \int_0^{t'} G(s)\{d\,[qsh_s(qs)]/\, ds\}\, ds \quad (18)$$

$$= qt' h_s(qt')\, G(t') - \int_0^{t'} \dot{G}(s)\, qsh_s(qs)\, ds \quad (19)$$

where

$$s = t - \xi; \quad t' = t + t_1 = \text{shearing time} \quad (20)$$

Differentiation of eq. (18) yields

$$\dot{\sigma}(t') = d\sigma(t')/\, dt' = G(t')\, d\{qt' h_s(qt')\}/\, dt' \quad (21)$$

With $\gamma(t') = qt'$, we get

$$\dot{\sigma}(t')/q = G(t')\, d\{\gamma h_s(\gamma)\}/\, d\gamma; \quad \text{where } \gamma = \gamma(t') \quad (22)$$

Since the damping function $h_s(\gamma)$ is unity for $\gamma = 0$ and decreases with γ, the product $\gamma h_s(\gamma)$ will show a maximum at some strain γ_{max}. For example, with eq. (12), we get $\gamma h_s(\gamma) = \gamma e^{-\mu\gamma}$ and the maximum is found at:

$$\gamma_{max} = 1/\mu \quad (23)$$

Wagner's theory thus predicts a maximum in the Mooney curve at a strain value independent of q; with $\mu = 0.1$–0.2, we get $\gamma_{max} = 5$–10.

In an actual Mooney test, we have[2] a rotation speed of 2 rpm, a rotor diameter of about 40 mm, and a height of the sheared rubber slab of about 2.5 mm. For the 4 min of rotation, the outer zone

is displaced by $2 \times 40 \times \pi \times 4 \approx 1000$ mm, which implies a shear of about 1000/2.5 = 400 and a shear rate q of 400/240 $\approx 1.67\ s^{-1}$. Consequently, the peak in Mooney torque at $\gamma_{max} = 1/\mu = 5$–10 occurs almost immediately after rotor start (after 1–2.5 s). In the actual rubber slab, the strain increases from zero at the rotation axis to a maximum at the outer side of the rotor. For simplicity, we only consider the maximum strains in the outer layers of the rubber slab. Corrections for the variation of strain over the slab can be made easily.

The apparent viscosity $\eta(t')$ is defined as $\sigma(t')/q$ and can be found from eq. (19). As an example, we apply the power law of eq. (4). For t' = 240 s, the strain is about 400. With μ = 0.1–0.2, this implies h_s values of $\exp(-400\ \mu) = e^{-40} - e^{-80}$ that can be neglected. Therefore, the first term in eq. (19) vanishes and with Eq. (4) and Eqs. (6.1.1) and (6.5.3) of ref. 13 we get

$$\sigma(t') = qnG_1 \int_0^{t'} s^{-n} \exp(-\mu q s)\, ds = nqG_1(\mu q)^{n-1}[\Gamma(1-n) - \Gamma(1-n,\ \mu q t')] \quad (24)$$

where $\Gamma(x)$ is the gamma function and $\Gamma(a, x)$ is the incomplete gamma function. A stationary state is reached for $\mu q t' \gg 1$; the incomplete Γ function then reduces to zero [according to eq. (6.5.32) of ref. 13, $\Gamma(a, x) \approx x^{a-1}\, e^{-x}$ for $x \gg 1$]; consequently, the stationary viscosity η_s is found as

$$\eta_s(q) = \sigma_{\mu q t' \to \infty}/q = nG_1(\mu q)^{n-1}\Gamma(1-n) \quad (25)$$

The Cox–Merz relation is only approximately obeyed. For the dynamic modulus $G_d(\omega)$ and viscosity $\eta_d(\omega) = G_d(\omega)/\omega$, the power-law model yields[4]

$$\eta_d(\omega) = G_1\Gamma(1-n)\omega^{n-1} \quad (26)$$

Therefore, the Cox–Merz ratio R, found from eqs. (25) and (26) equals

$$R = \eta(q)/\eta_d\ (\omega = q) = n\ \mu^{n-1} \quad (27)$$

Some numerical values are given in Table I; we observe that the ratio is on the order of but not equal to unity.

Table I Cox–Merz Ratio R for Various Values of n and μ

Slope n	μ = 0.1	μ = 0.2
0.25	1.41	0.84
0.50	1.58	1.12
0.75	1.33	1.12
1.00	1.00	1.00

Peak Stress. The ratio R' between peak stress [at $t' = 1/(\mu q)$] and steady-state stress can be found from eqs. (19) and (25). Of course, for the peak stress, we cannot neglect the first term in eq. (19). With $\mu q t'_{max} = 1$, this term becomes $(1/\mu)\ h_s(1) \times G(t'_{max}) = e^{-1}\ G(t'_{max})/\mu$. For the second term in eq. (19), we use eq. (24) with $\mu q t' = 1$. Adding both contributions, we get

$$\sigma_{max} = e^{-1}G(t'_{max})/\mu + nqG_1(\mu q)^{n-1}[\Gamma(1-n) - \Gamma(1-n,\ 1)] \quad (28)$$

With $G(t'_{max}) = G_1\ t'^{-n}_{max}$ and $t'_{max} = 1/(\mu q)$, we get

$$\sigma_{max} = n\ G_1 q^n \mu^{n-1}[e^{-1}/n + \Gamma(1-n) - \Gamma(1-n,\ 1)] \quad (29)$$

Together with eq. (25), this yields

$$R' = \sigma_{max}/\sigma_{\mu q t' \to \infty} = [e^{-1}/n + \Gamma(1-n) - \Gamma(1-n,\ 1)]/\Gamma(1-n) \quad (30)$$

Using the series expansion (6.5.29) and eqs. (6.5.2)–(6.5.4) of ref. 13, we get

$$R' = e^{-1}\{1/(n\Gamma(\alpha)) + 1/\Gamma(1+\alpha) + 1/\Gamma(2+\alpha) + 1/\Gamma(3+\alpha) + \cdots\} \quad (31)$$

where $\alpha = 1 - n$.

The function of eq. (31) is given in Table II. Equations (30) and (31) show that the peak ratio only depends on n and not on q or nonlinearity parameter μ, provided that $\mu q t' \gg 1$. The limiting behavior for $n \to 0$ or $n \to 1$ is readily understood. For $n \to 0$, we have $\alpha \approx 1$; the first term in eq. (31) (with $1/n$) becomes the leading one and we get $R' \approx e^{-1}/n$. For $n \to 1$, we have $\alpha \to 0$; $\Gamma(\alpha)$ becomes very large and the first term in eq. (31) vanishes. For the remaining terms, we take $\alpha \approx 0$ and find $\Gamma(k + \alpha) \approx \Gamma(k) = (k-1)!$,

Table II Ratio R' of Peak Stress and Steady-State Stress During the Mooney Test for Various Values of Small-Strain Stress–Relaxation Slope n

n	R'
0.1	4.12
0.2	2.30
0.3	1.71
0.4	1.42
0.5	1.26
0.6	1.16
0.7	1.09
0.8	1.05
0.9	1.02

with $k = 1, 2, 3, \ldots,$ ($x!$ denotes the factorial of x). Therefore, the series in eq. (31) becomes 1/1! + 1/2! + 1/3! + $\cdots = e$. Consequently, R' converges to unity for $n \rightarrow 1$ (see Table II). For practical elastomers, slope n often lies between 0.3 and 0.7; consequently, we expect R' values between about 1.09 and 1.7. Moreover, the n value generally decreases with increasing degree of chain branching or entanglements. Consequently, the peak value R' increases when the elastic effects become more dominant and R' can, in principle, be used as a measure for these effects. A comparison with experimental data is given in Figure 3. The height of the overshoot peak is predicted rather well. However, the scatter in the experimental data is too large to decide whether the trend of a decreasing R' with increasing n is really confirmed. A more comprehensive analysis appears necessary.

Mooney Stress Relaxation (t > 0)

We now have [see eqs. (13)–(15)]

$$\gamma(\xi) - \gamma(t) = \begin{cases} -\gamma_0 = -qt_1 & \xi < -t_1; \quad t > 0 \quad (32) \\ q\xi \quad -t_1 < \xi - t, < \xi < 0; & t > 0 \quad (33) \\ 0 \qquad\qquad 0 < \xi < t; & t > 0 \quad (34) \end{cases}$$

Substituting this into eq. (8), we get a formula similar to eq. (19):

$$\sigma(t) = \gamma_0 h_s(\gamma_0) G(t + t_1) - \int_0^{t_1} \dot{G}(t + s) qs\ h_s(qs)\ ds \quad (35)$$

where

$$s = -\xi \quad (36)$$

As before, the first term in eq. (35) can be neglected because of the very large strains. Taking the power law of eq. (4) and the damping function of eq. (12), we then get

$$\sigma(t) = nqG_1 \int_0^{t_1} se^{-ps}/(t + s)^{1+n}\ ds \quad (37)$$

where

$$p = \mu q \quad (38)$$

In this integral, ps runs from 0 at $s = 0$ to $pt_1 = \mu q t_1 = \mu\gamma_0 = 40$–$80$ at $s = t_1$. Therefore, the exponent becomes extremely small at $s = t_1$, which means that the upper limit of the integral can safely be changed into infinity

$$\sigma(t)/[n\ G_1\ q] = \int_0^{\infty} se^{-ps}/(t + s)^{(1+n)} = \int_0^{\infty} e^{-ps}/(t + s)^n\ ds - t \int_0^{\infty} e^{-ps}/(t + s)^{n+1}\ ds \quad (39)$$

Both standard integrals can be obtained from eq. (6.5.3) of ref. 13. We get

$$\sigma(t)/[nG_1q] = p^{n-1}e^{pt}[\Gamma(1 - n, pt) - pt\Gamma(-n, pt)] \quad (40)$$

where $\Gamma(a, x)$ is the incomplete gamma function discussed before. For $t = 0$, the result of eq. (25) is reproduced as

$$\sigma_0/[n\ G_1q] = \Gamma(1 - n)p^{n-1}; \quad \sigma_0 = \sigma\ (t = 0) \quad (41)$$

The relaxation ratio f is found as

$$f(z) = \sigma(z)/\sigma_0 = e^z\{\Gamma(\alpha, z) - z\Gamma(\alpha - 1, z)\}/\Gamma(\alpha) \quad (42)$$

where

$$z = pt = \mu qt \quad (43)$$

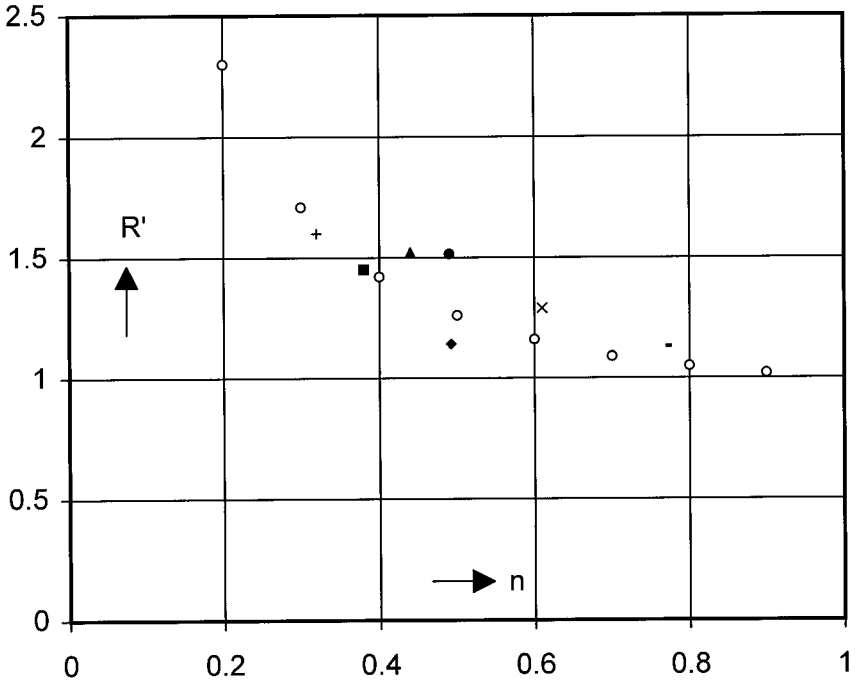

Figure 3 Overshoot ratio $R' = \sigma_{max}/\sigma_{stationary}$ versus slope $n = -d \ln G/d \ln t$ of the small-strain relaxation modulus at 125°C as calculated by eq. (31) (○) and as determined experimentally.[16] The experiments revealed that a reliable peak value is only found when the heating period preceding the Mooney test is taken much longer than the usual duration of 1 min (see ref. 8); here, a value of 10 min has been taken. The data refer to the following EPDM types:

Sample	M_w/M_n	ML (1 + 4) 125°C	n	R'
(●) A	≈ 4	34	0.49	1.52
(◆) B	2.8	37	0.49	1.14
(◆) C	≈ 4	47.5	0.44	1.52
(■) D	4.5	65	0.38	1.45
(×) E	3.8	74	0.61	1.29
(+) K	—	47	0.32	1.60
(−) L	—	46	0.77	1.13

$$\alpha = 1 - n \tag{44}$$

Clearly, the relaxation is a function of $z = \mu q t$ and $\alpha = 1 - n$ only (i.e., the shape of the relaxation curve on log t scale does not depend on μq and variations in μq shift the relaxation curve along the log t scale, without change in shape). Of course, this only holds as long as the nonlinear effects are very large and the first term in eq. (35) can be neglected.

An alternative for eq. (42) can be obtained by using recurrence formula (8.356.2) of ref. 14:

$$f(z) = \{(1 + z/n)e^z\, \Gamma(\alpha, z) - z^\alpha/n\}/\Gamma(\alpha) \tag{45}$$

A series expansion is obtained using function $\gamma^*(\alpha, z)$, defined in Section 6.5 of ref. 13. We have

$$\Gamma(\alpha, z)/\Gamma(\alpha) = 1 - z^\alpha \gamma^*(\alpha, z) \tag{46}$$

With eq. (45), this yields

$$f(z) = (1 + z/n)e^z - z^\alpha/[n\Gamma(\alpha)] - (1 + z/n)e^z z^\alpha \gamma^*(\alpha, z) \tag{47}$$

in which we can substitute the convergent series of eq. (6.5.29) of ref. 13,

$$f(z) = (1 + z/n)e^z - z^\alpha/[n\Gamma(\alpha)] - (1 + z/n)z^\alpha \sum_{k=0}^{\infty} z^k/\Gamma(\alpha + k + 1) \quad (48)$$

Special Cases

Small Values of z. The series of eq. (48) contains integral powers of z as well as fractional powers such as z^α. If $n < 1$, $\alpha = 1 - n$ is less than unity, and for $z \ll 1$, the fractional power z^α becomes the leading term. We then find

$$f(z) \approx 1 - z^\alpha/[n\Gamma(1 + \alpha)]; \quad z \ll 1; \quad 0 < \alpha = 1 - n < 1 \quad (49)$$

Large Values of z. The asymptotic expansion (6.5.32) of ref. 13 reads

$$\Gamma(\alpha, z) \approx z^{\alpha-1}e^{-z}[1 + (\alpha - 1)/z + (\alpha - 1)(\alpha - 2)/z^2 + \cdots]; \quad z \to \infty \quad (50)$$

in which $\alpha = 1 - n$, $\alpha - 1 = -n$, $\alpha - 2 = -(1 + n)$, etc. Substitution into eq. (45) yields

$$f(z)\Gamma(\alpha) = (1 + z/n)z^{\alpha-1}[1 - n/z + n(n + 1)/z^2 - n(n + 1)(n + 2)/z^3 + \cdots] - z^\alpha/n \quad (51)$$

or

$$nf(z)\Gamma(\alpha)z^{-\alpha} = (1 + n/z)[1 - n/z + n(n + 1)/z^2 - n(n + 1)(n + 2)/z^3 + \cdots] - 1 = n/z^2 - 2n(n + 1)/z^3 + \cdots \quad (52)$$

Therefore

$$f(z) \approx z^{-(1+n)}/\Gamma(1 - n); \quad \text{for } z \gg 1 \quad (53)$$

$$f(t) = \sigma(t)/\sigma_0 \approx (pt)^{-(1+n)}/\Gamma(1 - n); \quad pt \gg 1 \quad (54)$$

Consequently, at large values of t, the stress relaxes with power $-(1 + n)$ that is one unit higher than that of the small-strain stress relaxation. This unexpected result, which may be due to the simplifications implied in eqs. (4) and (12), also follows from eq. (39). For large p values, the exponent has already decreased to zero before the function $(t + s)^{-(1+n)}$ begins to deviate from its value $t^{-(1+n)}$ at $s = 0$. Therefore, this function may be taken outside the integral and we obtain

$$\sigma(t)/[nG_1q] = t^{-(1+n)} \int_0^\infty se^{-ps}\, ds = t^{-(1+n)}/p^2 \quad (55)$$

With eq. (41), this reproduces eq. (54). The accuracy of the approximations of eqs. (53) and (54) can be estimated by considering the ratio of the second and first term in the expansion of eq. (52); we find a ratio of $2(1 + n)/z$. At $z = 10$ and $n < 1$, the approximation is to within 40%; for $z > 100$, and $n < 1$, to within 4%.

COURSE OF MOONEY STRESS RELAXATION

Ratio $f(z)$ versus z, as calculated with eq. (48), is given in Figure 4. We observe the following.

1. Due to the strong nonlinear effects, the relaxation is much faster than in the linear case (Fig. 2). For μ between 0.1–0.2 (as for PE[7]), the q value of 1.67 s^{-1} in the Mooney test leads to a $p = \mu q$ value of 0.17–0.34 [i.e., we have z/t = 0.17–0.34 [c.f., eq. (43)]. Thus, the t range up to 10 s as practiced in Mooney Stress Relaxation tests corresponds to maximum z values of 1.7–3.4. Figure 4 shows that for common n values (0.2–0.8), most of the stress has relaxed within this period. Thus, it is the nonlinear effects that are responsible for the rapid Mooney Stress Relaxation.
2. The higher the value of n, the faster the relaxation is. Therefore, the more elastic the polymer melt or elastomer, the slower the Mooney relaxation. The relaxation rate can be characterized by z_{80} or z_{50} (i.e., by the time, z, at which σ has relaxed to 100 − 80 = 20% or to 100 − 50 = 50% of the original value σ_0). Plots of these time parameters as functions of n are given in Figure 5; obviously, z_{50} or z_{80} correlate well with n. The same applies to the more common Mooney-relaxation parameters t_{80} or t_{50}, which are proportional to z_{80} and z_{50} [$t_x = z_x/(\mu q)$; see eq. (43)].
3. Figure 4 further shows that the Mooney Stress Relaxation does not obey a power law. The lines are strongly curved and only at large z values is a final slope of $-(1 + n)$ reached. This suggests that a treatment of Mooney Stress Relaxation by a power

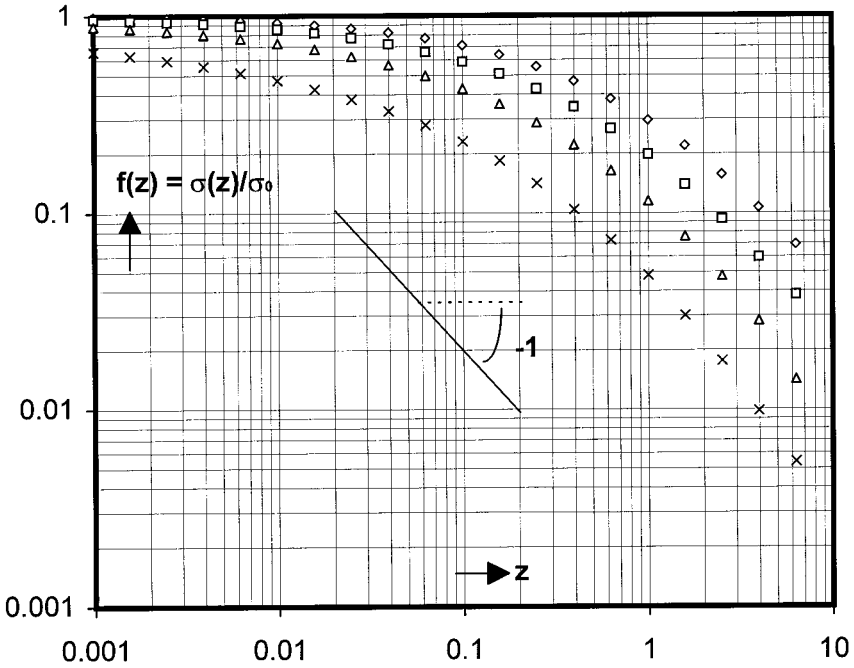

Figure 4 $f(z) = \sigma(z)/\sigma_0$ versus $z = \mu q t$ in Mooney Stress Relaxation for $n = 0.2$ (◇), 0.4 (□), 0.6 (△), and 0.8 (×) as calculated with eq. (48). The slope at $z \rightarrow \infty$ equals $-(1 + n)$ [see eq. (53)]; the slope of -1 is as indicated. For the z range of practical Mooney Stress Relaxation tests ($z < 1.7$–3.4; see text), the limiting slope of $-(n + 1)$ has not been reached in all cases.

law[1–2] should be considered as an approximation, valid for a narrow time interval only. We further observe that the slope increases with time.

4. Figure 4 and eq. (48) finally show that the shape of the f versus $\log z$ or $\log t$ curve is independent of deformation rate q and nonlinearity parameter μ. The only effect of q and μ is to shift the relaxation curve along the $\log t$ scale (i.e., the higher $q\mu$, the faster the relaxation on $\log t$ scale). As said before, this only holds as long as the nonlinearities are sufficiently strong [i.e., the first term in eq. (35) can be neglected].

So far, for the theoretical treatment of Mooney Stress Relaxation, verification, using experimental data on EPDM rubbers with widely varying properties, is given in Part II of this series.[8]

ACCURACY OF MOONEY STRESS RELAXATION SLOPE, t_{80}, AND SURFACE A

We now investigate which of the three parameters is the most accurate. We consider the $M(t)$ versus t curve (Fig. 1) and assume that (i) the only experimental error is a random variation δM in $M(t)$ with a magnitude less than some quantity Δ, independent of time (i.e., $|\delta M| < \Delta$), (ii) the real course (no errors) of M follows a power law with negative slope $-a$ (a is taken positive). As shown in the previous section, a power law can only be an approximation. As will be clear from the text, such an approximation suffices for the purpose of

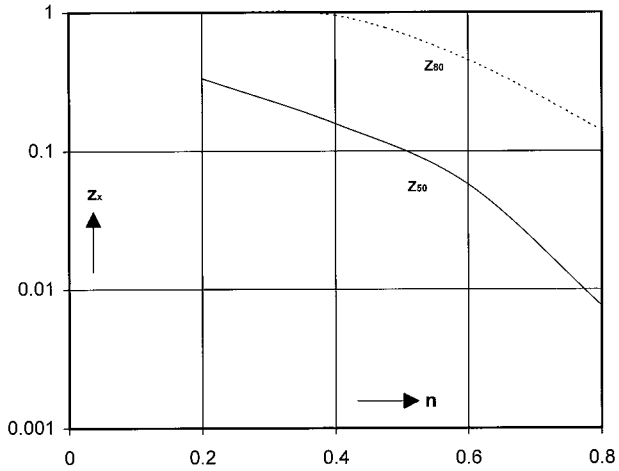

Figure 5 z_{80} and z_{50} as function of the slope n of the small-strain stress relaxation.

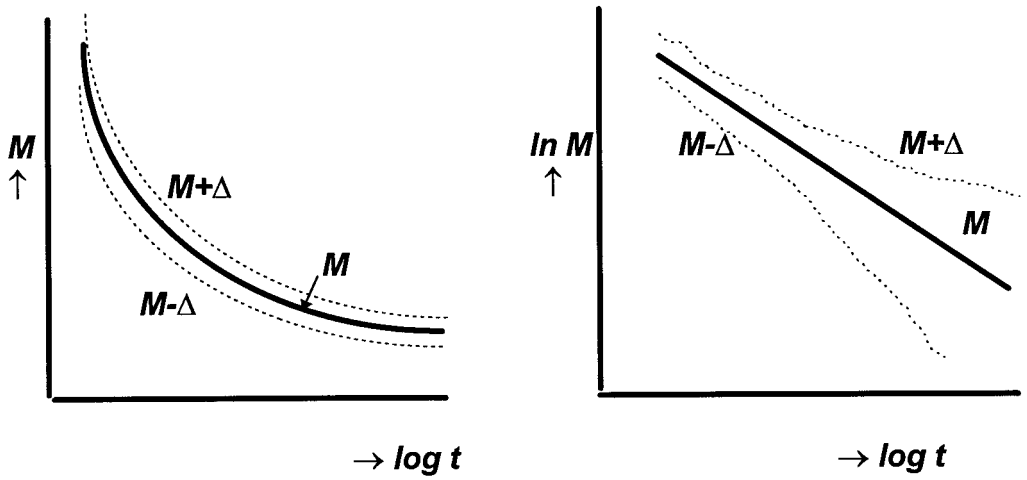

Figure 6 Effect of a time-independent error Δ on the plots of M and ln M versus log t. Because of the decrease of M with time, the relative error in M and the absolute error in ln M increase with time.

the present error analysis. The M versus t curve is supposed to be measured between times t_1 (e.g., 1 s) and t_2 (e.g., 10 s). The values of M at t_1 and t_2 are denoted by M_1 and M_2, respectively; M_1 is called the intercept.[2] We further define time t_x as the time at which $M(t_x)/M_1$ has decreased to $1 - x$. Thus, our $t_{0.8}$ can be compared with the time, t_{80}, used in the literature[2,12] and more general, our t_x with the t_{100x} parameter from literature. The only difference is that we define t_x on the basis of the value, M_1, measured at the shortest time t_1; usually, t_x is defined on the basis of the Mooney value, M_0, at rotor stop. For the purpose of error analysis, this difference is considered insignificant.

Since $M(t)$ decreases with time, the random absolute variation δM with amplitude, Δ, leads to a relative error $\delta M/M(t)$ that increases with time. For example, for $x = 0.8$, the relative error in M at $t_{0.8}$ is five times larger than that at t_1. Denoting the relative error at t_1 by $\varepsilon = \Delta/M_1$, the relative error at t_x equals $\varepsilon/(1 - x)$. Since the analysis of the Mooney Stress Relaxation data is generally based on a log–log plot of M versus t, we have to consider the errors in ln M. For small errors, the absolute error $\delta \ln M$ in ln M equals the relative error, $\delta M/M$, in M; we will use this simplification throughout. Thus, the absolute error in ln M increases with time as illustrated in Figure 6.

The errors in intercept, slope, surface, and t_x are found as follows.

Intercept (i.e., the value of M *and* $t = t_1$*).* According to our definitions, the relative error $\delta M/M$ for $M = M_1$ equals $\varepsilon = \Delta/M_1$. Note that we considered the time values as error free (i.e., we assumed that the rotor stop was instantaneous; an ill-defined slow-down period induces additional errors, particularly at short times).

Time t_x. Since the double log slope equals $-a$, we have $\delta \ln M/\delta \ln t = -a$. Since the relative error in M at t_x as well as the absolute error $\delta \ln M$ in ln M are equal to $\varepsilon/(1 - x)$, the relative error in t_x is given by:

$$\delta t_x/t_x = \varepsilon/[a(1 - x)] \tag{56}$$

Obviously, the error in t_x is considerably larger than that in the intercept. [Example: for $x = 0.8$ and $a = 0.5$, we get an error of 10ε (ten times that of the intercept)]. The error becomes greater the smaller slope a is and the more x approaches unity. Clearly, t_x is not an accurate quantity and the proposal to use t_{80}[12] (our $t_{0.8}$) needs reconsideration; t_{50} is 2.5 and t_{40} is 3 times more accurate.

Slope. The error can be calculated as shown in Figure 7. In the absence of errors we have line a given by:

$$\text{line a:} \quad \ln M = \ln M_1 - ay; \quad y = \ln(t/t_1) \tag{57}$$

Line b is the upper possibility with all errors equal to $+\Delta = \varepsilon M_1$. The relative error in $M(t)$ then equals $+\varepsilon\ M_1/M(t) = \varepsilon(t/t_1)^a = \varepsilon\ e^{ay}$. Since, for small errors, the absolute error in ln M equals the relative error in M, line b is given by:

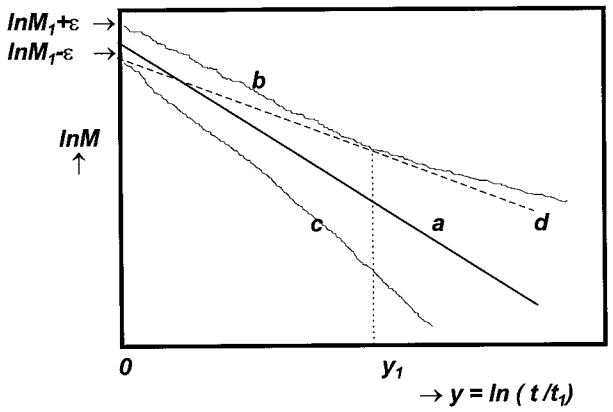

Figure 7 Effect of errors on the slope. Line a, eq. (57), refers to zero errors, line b to maximum positive errors, line c to maximum negative errors. Line d [Eq. (60)] is the straight line with the lowest possible slope that passes throughout the error band. It touches the point $\ln M_1 - \varepsilon$ at $y = 0$ and the line b (upper boundary) at $y = y_1$. The error zone widens for $y \to \infty$; therefore, the minimum slope is not sensitive to the large errors in ln M at large y values.

$$\text{line b:} \quad \ln M = \ln M_1 - ay + \varepsilon e^{ay} \tag{58}$$

In the same way, the minimum course is given by:

$$\text{line c:} \quad \ln M = \ln M_1 - ay - \varepsilon e^{ay} \tag{59}$$

Line d is the straight line with minimum slope, p, that passes through the error zone. It goes through the lowest ln M value at $y = 0$ ($t = t_1$; ln $M = \ln M_1 - \varepsilon$) and touches upper line b at some point y_1 (see Fig. 7). The formula is

$$\text{line d:} \quad \ln M = \ln M_1 - \varepsilon - py \tag{60}$$

The value of p can be found from the condition that, at $y = y_1$, the M values as well as the slopes, $d \ln M/dy$, of lines b and d should be equal. Consequently,

$$-ay_1 + \varepsilon \exp(ay_1) = -\varepsilon - py_1; \quad \text{equal } M \text{ values} \tag{61}$$

$$-a + \varepsilon a \exp(ay_1) = -\text{p}; \quad \text{equal slopes} \tag{62}$$

Writing $z = ay_1$, eqs. (61)–(62) yield $z = 1 + e^{-z}$, which has the solution $z = 1.2785$. Substituting this in eqs. (61)–(62), we find

$$(a - p)/a = 3.6\ \varepsilon \tag{63}$$

Consequently, the minimum slope is $1 - 3.6\varepsilon$ times the slope, a, in the absence of errors. In the same way, we find a maximum slope of $(1 + 3.6\varepsilon)a$. Altogether this means that the relative error in slope is given by:

$$\delta a/a = 3.6\ \varepsilon \tag{64}$$

As is clear from Figure 7, the error in the slope is not sensitive to the large errors in ln M at large t/t_1 values. Further, the error in slope seems independent of the length of the time interval over which the Mooney Stress Relaxation is measured, which contradicts the well-known fact that errors in slope increase with decreasing length of the time interval. The explanation is that we assumed that the curve was measured up to at least the point y_1 (Fig. 7). Since $z = ay_1 = 1.2785$, $y_1 = \ln(t/t_1)$ must exceed $1.2785/a$ (i.e., a minimum length has been assumed implicitly and the minimum time interval increases with $1/a$).

Ratio, R, of the relative errors in t_x and slope a is found from eqs. (64) and (56):

$$R = [\delta t_x/t_x]/\delta a/a = 1/[3.6a(1 - x)] \tag{65}$$

The ratio increases with $1/a$ and $1/(1 - x)$; some numerical values are given in Table III. Obviously, the t_{80} parameter is always less accurate than the slope. As said before, the parameters t_{50} and t_{30} are, respectively, 2.5 and 3 times more accurate.

Surface. According to ref. 2, A is the surface area under the M versus t curve (linear plot) between t_1 and t_2. Assuming t_1 and t_2 are fixed and error-free, the error in A equals

$$\delta A = (t_2 - t_1)\Delta \tag{66}$$

For a power law with slope $a \neq 1$ and initial value M_1 at t_1, the surface is given by:

Table III Ratio, R, of Relative Errors in t_x and Slope a According to eq. (65) for Three Values of x, as a Function of Slope a

a	t_{30}	t_{50}	t_{80}
0.2	1.99	2.78	6.95
0.4	0.99	1.39	3.47
0.6	0.66	0.93	2.32
0.8	0.50	0.69	1.74
1.0	0.40	0.55	1.39

Table IV Ratio R' of the Relative Errors in Surface and Slope According to eq. (69) for Two Values of $r = t_2/t_1$; Numbers in Parentheses Give the Fractional Stress, r^{-a}, at the End of the Relaxation Period

a	$r = 10$	$r = 100$
0.2	0.38 (0.63)	0.57 (0.40)
0.4	0.50 (0.40)	1.11 (0.16)
0.6	0.66 (0.25)	2.07 (0.063)
0.8	0.86 (0.16)	3.64 (0.025)
1.0	1.25 (0.10)	6.88 (0.010)

$$A = [t_1 M_1/(1 - a)][(t_2/t_1)^{1-a} - 1] \quad (67)$$

Combining eqs. (66) and (67) with $\varepsilon = \Delta/M_1$, we find for the relative error:

$$\delta A/A = \varepsilon(1 - a)[r - 1]/[r^{1-a} - 1]; \quad r = t_2/t_1 > 1 \quad (68)$$

The ratio $R' = [\delta A/A]/[\delta a/a]$ is found from eqs. (64) and (68):

$$R' = (1 - a)(r - 1)/[3.6(r^{1-a} - 1)] \quad (69)$$

Some numerical values are given in Table IV. We observe that the errors in surface increase with a and r. For $r = 100$, the errors in surface are larger than those in slope for $a > 0.4$; for $r = 10$, they are smaller or about equal.

We can compare the present results with those of a round robin test.[15] These tests had a t_2 value of 100 s and a t_1 between 1 and 2 s (not accurately known). Thus, $r = 100$ for $t_1 = 1$ s and 50 for $t_1 = 2$ s. The measured slope values for rubbers F-I are given in the second column of Table V and range between 0.4 and 0.8. Since r is on the order of 100, Table IV suggests that the error in surface will be larger than that in slope. The measured ratio of the relative coefficient of variation in surface and slope is given in the third column. As suggested by the above error analysis, the relative errors in the surface are larger than those in the slope. The ratio calculated with eq. (69) is given in the fourth and fifth columns, for $t_1 = 1$ s and $t_1 = 2$ s, respectively.

Summarizing, the relative errors increase in the order of intercept, slope, t_{80}. For a slope between 0.2 and 1, the errors in t_{80} are 1.4–7 times larger than those in the slope. The errors in surface depend on the t_2/t_1 ratio; for $r = 100$, the surface is less accurate, for $r = 10$, the surface is more accurate than the slope.

This result is not surprising. As shown in Figure 8, the errors in ln M increase with increasing time. A quantity such as t_{80} is solely determined by the long-time ln M values and is, therefore, the least accurate. Surface A is determined by the $M(t)$ values over the whole range and has an average accuracy. The slope is determined by the shorter time values and is better than t_{80}. The most accurate is the intercept, because it is determined by the shortest time value, $M(t_1)$ of $M(t)$; however, this intercept gives no information about the relaxation rate.

CONCLUSIONS

1. Mooney Stress Relaxation cannot be described by linear viscoelastic theory; this theory fails in explaining the very existence of a rapid relaxation (e.g., in 10 s after 4 min of shearing).
2. Mooney viscosity and Mooney Stress Relaxation can be described by Wagner's nonlinear rheological theory.

Table V Ratio R' of the Relative Errors in Surface A and Slope a

		Ratio R'		
			Theory, Eq. (69)	
Material[15]	Slope a[15] Experimental	Experimental[15]	$t_1 = 1$ s	$t_1 = 2$ s
F	0.41	1.65	1.2	0.9
G	0.82	1.52	3.8	2.4
H	0.68	1.41	2.6	1.7
I	0.74	1.65	3.1	2.0

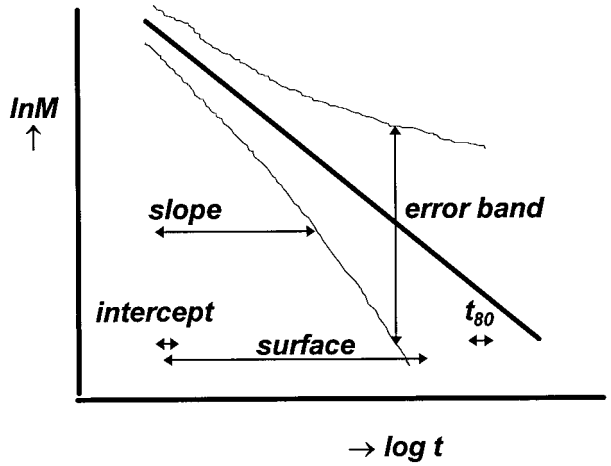

Figure 8 Explanation of the different accuracy in intercept, slope, etc. The (assumed) exact course of $M(t)$ is given by the thick line, the thin curves give the upper and lower boundary of the error zone, the errors in ln M increase with time. The arrows indicate the time ranges that determine intercept, slope, surface, and t_{80}; schematical.

3. The peak in the Mooney (shearing period) occurs just after rotor start; its height is 1–2 times the steady-state value of the stress. The peak increases with increasing elasticity (i.e., decreasing value of small-strain double-logarithmic stress-relaxation rate n). The peak may be used as a measure for the elastic effects in unvulcanized elastomers.
4. As compared to the small-strain case, the nonlinearities highly accelerate the Mooney Stress Relaxation after rotor stop.
5. The double-logarithmic slope, $-m$, of the Mooney Stress Relaxation curve, is not identical to the slope, $-n$, at small strains; for $t \to \infty$, we have $m = n + 1$.
6. The Mooney Stress Relaxation is not a straight line in a double log plot; a power-law approximation will only be valid over a narrow time range.
7. Mooney Stress Relaxation is faster for the larger slope, n; quantities such as t_{50} or t_{80} correlate well with n and can be used for quality control; however, because of experimental inaccuracies, t_{50} or t_{40} are to be preferred over the inaccurate quantity t_{80}.
8. Generally, the accuracy decreases in the order of intercept, slope, t_{80}.

Conclusions 3, 5, 6, and the first part of 7 refer to small-strain relaxation according to a power law with exponent n and a damping function with one exponent only.

REFERENCES

1. Koopmann, R.; Kramer, H. J Test Eval 1984, 12(6), 407.
2. ASTM D 1646. Annu Book ASTM Stand 1996, p 328–337.
3. Vennemann, N.; Lüpfert, S. Kautschuk + Gummie + Kunststoffe 1991, 44, 270.
4. Ferry, J. D. Viscoelastic Properties of Polymers, 3rd ed.; Wiley: New York, 1980.
5. Wagner, M. H. Rheol Acta 1976, 15, 133; Rheol Acta 1977, 16, 43.
6. Wagner, M. H. J Non-Newtonian Fluid Mech 1978, 4, 39.
7. Schwarzl, F. R. Polymer-Mechanik; Springer: Berlin, 1990.
8. Steeman, J. Appl Polym Sci, Part II of this series.
9. Beelen, H. J. H.; Maag, L. R. Presented at the 1996 International Rubber Conference, Manchester, UK.
10. Beelen, H. J. H. Presented at the 1997 International Rubber Conference, Nürnberg, Germany.
11. Meijers, P. W. L. J.; Maag, L. R.; Beelen, H. J. H.; van der Ven, P. M. Presented at the meeting of the Süd-Deutsches Kunststoff-Zentrum, Würzburg, Germany, October 1997.
12. Friedersdorf, C. B.; Duvdevani, I. Rubber World 1995; p 30, January.
13. Abramowitz, M.; Stegun, I. A. Handbook of Mathematical Functions, Dover: New York, 1972.
14. Gradshteyn, I. S.; Ryzhik, I. M. Tables of Integrals, Series and Products, Academic Press: New York, 1980.
15. Noordermeer, J., DSM Elastomers, unpublished results, (1997).
16. Boerstoel, H., Internal Report DSM Research, 1985, unpublished report.